CHAPTER V

CONVERSION OF METHYLESTERS TO HYDROCARBONS OVER Zn-MODIFIED H-ZSM5 ZEOLITE CATALYST*

5.1 Abstract

The conversion of methyl octanoate, a model fatty acid methyl ester, has been studied on Zn/H-ZSM5 and H-ZSM5 catalysts. Deoxygenation, coupling, cracking, and aromatization reactions take place under the reaction conditions investigated. These reactions are relevant to the refining of fuels derived from biomass containing triglycerides, such as vegetable oils and algae. While the addition of Zn to H-ZSM5 has a significant promoting effect in the aromatization of light alkanes, the effect is much lower when the feed is a methyl ester. This difference may be related to the different reaction paths that occur in the aromatization of alkanes and methyl esters, respectively. The experiments conducted with n-octane indicate that aromatics are produced through a series of consecutive reactions that include cracking, oligomerization, and cyclization. In this case, the addition of the Zn leads to a more effective aromatization than that obtained with the H-ZSM5. By contrast, the conversion of methyl octanoate proceeds via condensation reactions leading to the formation of large ketones and esters, which subsequently crack at the oxygenated function and C_7 hydrocarbons and aromatics as secondary products. In this case, the presence of Zn does not provide enhance the aromatization path nor provides any alternative reaction paths for aromatization. Moreover, direct ring closure via activation of C next to the CO group has been identified.

Keywords: Biofuels; Methyl ester conversion; Alkane conversion; Aromatization; Zn/H-ZSM5

---

* Catalysis Letters, In press

5.2 Introduction

Although fatty acid methyl esters (FAMEs) obtained from the transesterification of triglyceride with methanol have received significant attention as a renewable diesel fuel [1-3], the presence of oxygen in the molecule induces oxidative and thermal instability and lowers its heating value [4-6]. Therefore, the elimination of oxygen from FAMEs has been extensively investigated particularly on metal catalysts, such as Pd/C, and CoMo- and NiMo-supported Al_2O_3 [7-10]. High hydrogen pressures are typically required to effect the deoxygenation and keep the catalyst active. An alternative path that can occur under milder conditions is via the use of acidic zeolites such as H-ZSM5, which can convert oxygenates into aromatics and other gasoline components. For instance, H-ZSM5 zeolite has been successfully used as a catalyst to transform aldehydes, ketones, and acids into hydrocarbons [11,12]. In generally, it has been reported that oxygenates can be converted first to olefins and then to aromatics at high enough temperatures to effect decarbonylation, decarboxylation, and dehydration. Our own previous study has shown H-ZSM5 is an effective catalyst for conversion of FAMEs [13]. We found that the conversion of methyl octanoate on H-ZSM5 yields a range of C_1–C_7 hydrocarbons with significant amounts of aromatics. The product distribution analysis showed that octanoic acid and 8-pentadecanone are early products. It is possible that hydrolysis of the ester produces the acid, which then undergoes decarboxylative ketonization to form the C_{15} condensation product. At higher W/F, these primary products undergo a series of consecutive reactions that produce aromatics. In this contribution, we have explored the use of Zn as a promoter to enhance the aromatization capacity of the catalyst. It is well known that addition of Zn to H-ZSM5 greatly enhances the aromatization of light alkanes [14-19]. Therefore, we have investigated the conversion of methyl octanoate, a FAME model compound, over a Zn-modified H-ZSM5 zeolite catalyst (Zn/H-ZSM5) in comparison to the unpromoted H-ZSM5.

5.3 Experimental

5.3.1. Catalyst Preparation

The parent ZSM5 zeolite was prepared by using the conventional hydrothermal technique [20], using tetrapropylammoniumbromide (TPABr) as the organic template. The synthesized zeolite (NaZSM5) was calcined at 873 K for 5 h to remove the organic templates. Subsequently, the NaZSM5 zeolite was cation-exchanged to NH_4ZSM5 using 1 M of NH_4NO_3 solution at 353 K for 10 h. The resulting solid was separated from the solution by filtering and washing. The exchange procedure was repeated three times to complete the ion exchange. After this step, the sample was dried overnight at 383 K and calcined in flowing dry at 773 K for 5 h to produce the acidic form of the zeolites (H-ZSM5). The Zn-containing zeolite (Zn/H-ZSM5) was prepared by ion-exchange of the H-ZSM5 with a $Zn(NO_3)_2$ solution (0.005 M) at 353 K for 5 h. The exchanged samples were dried overnight at 383 K and calcined at 773 K for 5 h.

5.3.2 Catalyst Characterization

XRD was used to characterize the structure of the zeolite using a Rigaku X-Ray Diffractometer. The crystal morphology and crystal size were investigated in a JEOL 5200-2AE SEM. The surface areas were obtained by nitrogen adsorption at 77 K using a Thermo Finnigan Modeled Sorptomatic 1100 series. Elemental analyses were carried out in a Perkin-Elmer Optima 4300 DV Inductively Coupled Plasma optical emission spectrometer (ICP-OES).

The acidity of the catalysts was quantified by the amine TPD (Temperature Programmed Desorption) technique developed by Gorte *et al.* [21]. Prior to the amine adsorption, the sample (30 mg) was pretreated in flow of He for 1 h at 773 K. Then, the sample was cooled to room temperature, and 10 μl pulses of liquid propylamine were vaporized and injected over the sample until the sample was saturated. The saturation of the propylamine adsorption was monitored by mass spectrometry. Excess propylamine was removed by flowing He for 3 h. The sample

was then linearly heated at a ramping rate of 10 K/min to 973 K. Masses (m/e) 30, 41, and 17 were monitored to determine the evolution of propylamine, propylene, and ammomia, respectively. The amount of propylene desorbed was calibrated with a 5-ml pulse of 2% propylene in He.

The number and strength of acidic sites of the catalyst were characterized by FTIR using pyridine as a probe molecule. Infrared spectroscopic measurements of the adsorbed pyridine (Py-IR) were recorded on a Bruker Equinox 55 spectrometer. The self-supported wafer sample (~90 g) was placed in a gas-tight cell with CaF_2 windows. Initially, the sample was pretreated in He flow at 773 K for 2 h. Then, it was cooled to 423 K, and a blank spectrum was taken. Saturated pyridine vapor was introduced into the cell for 2 h in order to saturate the acid sites. The excess pyridine was then purged from the cell by flowing He for 12 h. Four spectra were obtained for each sample at 423 K, both on the saturated sample, and after outgassing at increasing temperatures from 573 to 773 K. The density of both BrØnsted and Lewis acid sites was quantified by integrating the corresponding absorption bands and using published molar extinction coefficients [22].

5.3.3 Catalytic Activity Measurement

The conversion of methyl octanoate (MEO, Sigma-Aldrich) was carried out in a ¼ inch quartz single-pass continuous flow reactor, packed with catalyst powder, and operating in the gas phase at 773 K under atmospheric pressure. To investigate the product distribution as a function of methyl octanoate conversion, the space time (W/F) was varied from 0.8 to 25.4 $g_{cat}.h/mol_{MEO}$. The catalysts were first pretreated *in situ* for 1 h in flowing H_2 at the reaction temperature. Methyl octanoate was then injected using a syringe pump through a heated vaporization port. The H_2 to feed molar ratio employed in all the experiments was 6:1. The products were analyzed by online gas chromatography (Shimadzu GC-17A) using a temperature program to optimize product separation and a GC/MS (Shimadzu Q5000) for product identification.

5.4 Results and Discussion

5.4.1 Catalyst Characterization

The H-ZSM5 and Zn/H-ZSM5 were characterized by XRD, SEM, and BET. The XRD patterns for both catalysts were almost the same and consistent with those reported in the literature for a typical H-ZSM5, confirming that the Zn/H-ZSM5 contains the same crystalline phase after zinc loading by ion exchange. The ICP chemical analysis, the approximate crystallite size determined by SEM, and the pore volume of the H-ZSM5 and Zn/H-ZSM5 are summarized in Table 5.1. The chemical analysis indicates that the amount of Zn in the Zn/H-ZSM5 catalyst is 0.3 wt%. This metal content resulted in a slight drop in pore volume and BET surface area relative to the H-ZSM5 catalyst.

Table 5.1 Physical properties of the H-ZSM5 and Zn/H-ZSM5 catalysts

	H-ZSM5	**Zn/H-ZSM5**
Si/Al from chemical analysis	36	36
Zn content (%wt)	0	0.3
Pore Volume (cm^2/g)	0.26	0.24
Particle size (μm) from SEM	~ 3	~ 3
Brønsted acidity density (μmol/g_{cat}) from TPD of propylamine	382	218

A more significant drop (~42%) upon Zn incorporation was observed in the Brønsted acid density determined by TPD of propylamine. A comparable decrease in Brønsted site density was observed by FTIR of adsorbed pyridine (~38%), as shown in Table 5.2. It is interesting to compare these estimates in the drop in number of acid sites with the number of Zn cations incorporated (45.8 μmol/g) in the catalyst. With two H^+ sites per Zn^{2+} cation, the loss in Brønsted acid density should have been only

about 24%. This difference is probably due to the much larger size of the Zn cation than the proton, blocking some of the zeolite channels and making some of the remaining acid sites inaccessible to the adsorption of propylamine. By contrast, the density of Lewis acid sites increased as a result of the presence of Zn, as previously reported [23,24].

Table 5.2 Acidity characterization of the H-ZSM5 and Zn/H-ZSM5 catalysts using the FTIR of adsorbed pyridine

	Acidity (μmol Py/g_{cat})							
	Brønsted (1545 cm^{-1})				**Lewis (1445 cm^{-1})**			
	423 K	**573 K**	**673 K**	**773 K**	**423 K**	**573 K**	**673 K**	**773 K**
H-ZSM5	176	90	48	35	37	11	8	5
Zn/H-ZSM5	92	73	42	9	88	39	18	11

5.4.2 Conversion of Methyl Octanoate

The conversion of methyl octanoate at 773 K as a function of time on stream is shown in Figure 5.1 for the H-ZSM5 and Zn/H-ZSM5 catalysts. In both cases, the initial activity was very high and under these conditions there was excess catalyst, converting 100% of the feed. Lower conversions can be observed at longer times on stream or at higher W/F. Operating at high conversions is not the best for comparing relative activities, but it is necessary when one needs to investigate the product distribution when the products of interest are not primary. Table 5.3 summarizes the product distributions obtained from the reaction of methyl octanoate over the H-ZSM5 and the Zn/H-ZSM5 catalysts after 20 min and 410 min on stream, which result in high and intermediate levels of conversion, respectively. When the conversion is high, at the beginning of the reaction (e.g. 20 min TOS), the selectivity to aromatics (benzene, toluene and C_8 aromatics) is about the same for both Zn/H-

ZSM5 and H-ZSM5 catalysts. In fact, the whole product distribution is rather similar for both catalysts, with some differences in the C_4-C_8 hydrocarbon range that is higher for the Zn/H-ZSM5 catalyst and particularly the presence of octanoic acid and 8-pentadecanone, which is higher on H-ZSM5. After several hours on stream, the catalysts deactivate with a consequent decrease in selectivity to aromatics. The Zn/H-ZSM5 is seen to produce mainly the condensation product, pentadecanone, which may be responsible for the more rapid deactivation of this catalyst compared to the unmodified H-ZSM5.

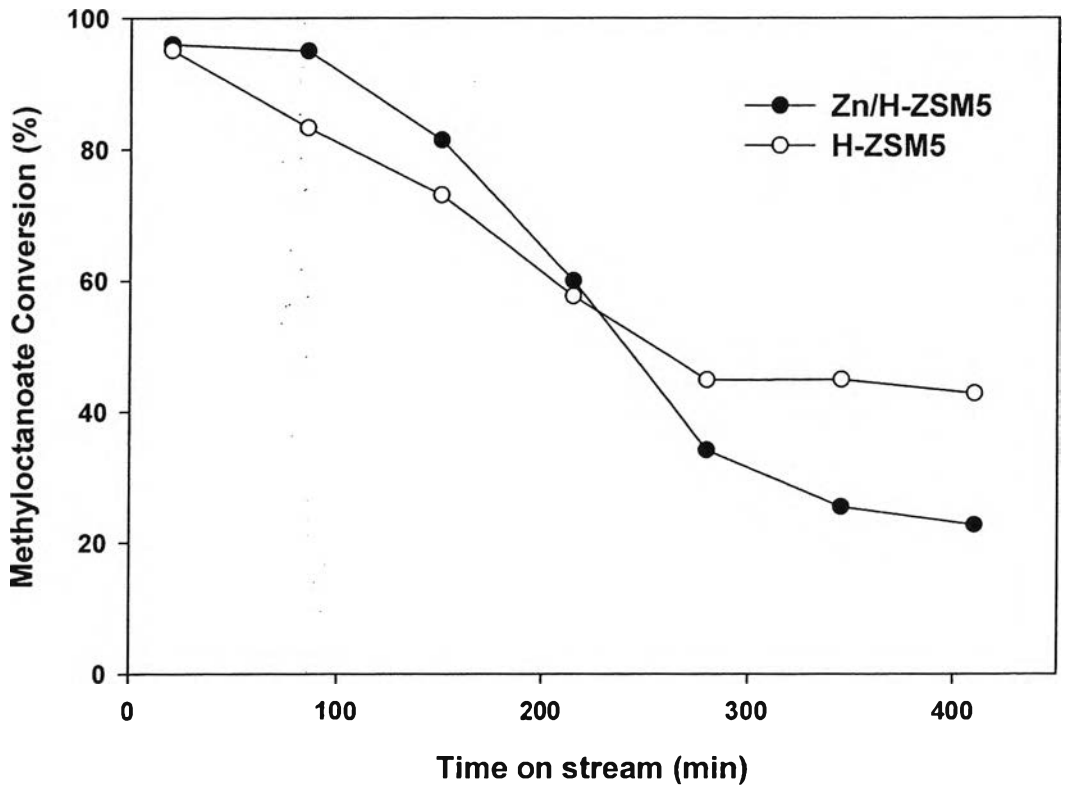

Figure 5.1 Conversion of methyl octanoate over the H-ZSM5 and the Zn/H-ZSM5 catalysts as a function of time on stream at 773 K under atmospheric pressure with W/F = 3.2 g*h/mol.

Table 5.3 Product distributions from the reaction of methyl octanoate on the H-ZSM5 and Zn/H-ZSM5 catalysts

	H-ZSM5		Zn/H-ZSM5	
Time on stream (min)	20	410	20	410
Conversion (%)	95.0	43.3	96.5	22.8
Product Selectivity (wt%)				
Methane	3.4	1.2	3.5	1.9
C_2	30.9	27.3	30.2	0.7
C_3	14.2	11.4	13.5	3.4
C_4	1.5	1.9	4.1	0.1
C_5	7.4	7.8	13.2	0.8
C_6	3.6	4.5	8.3	2.0
C_7	3.8	11.4	8.8	12.1
Benzene	0.9	1.1	1.1	0.0
Toluene	3.0	0.9	3.9	0.1
C_8 aromatics				
Ethylbenzene	0.7	0.4	1.0	0.0
m-Xylene	5.0	2.1	5.4	0.0
p-Xylene	0.8	0.3	0.8	0.2
o-Xylene	0.2	0.9	0.0	0.7
C_9+ aromatics	2.4	1.6	1.7	0.6
Total Aromatics	13.0	7.3	13.9	1.6
Octanal	0.7	0.3	0.4	0.0
Octanoic acid	14.5	14.7	1.0	9.4
Coupling Products				
Pentadecene	0.9	1.5	1.3	5.1
8-pentadecanone	6.0	10.4	1.7	60.0
Coupling ester	0.1	0.3	0.1	2.9

Reaction Conditions: 773 K, 1 atm, W/F = 3.2 g*h/mol, and H_2:Feed = 6:1 molar ratio

To identify the primary and secondary products obtained from methyl octanoate over the Zn/H-ZSM5 catalyst the evolution of yield for various product are shown as a function of W/F in Figure 5.2. It can be clearly observed that aromatics are secondary products since the derivative of aromatics yield with respect to W/F is zero at low W/F. On the other hand, condensation products such as 8-pentadecanone and coupling esters appear to be the primary products, which increase initially with increasing W/F and then decrease as they are consumed by further reactions. The 8-pentadecanone is most likely produced by acid-catalyzed decarboxylative ketonization [25] and the tetradecenes from the deoxygenation of 8-pentadecanone, which may involve hydrogenation/dehydration as proposed by Dumesic et al. [26, 27]. The decrease in the concentration of pentadecanone and tetradecenes with the W/F indicates that they undergo further reaction to either cracking products or aromatics.

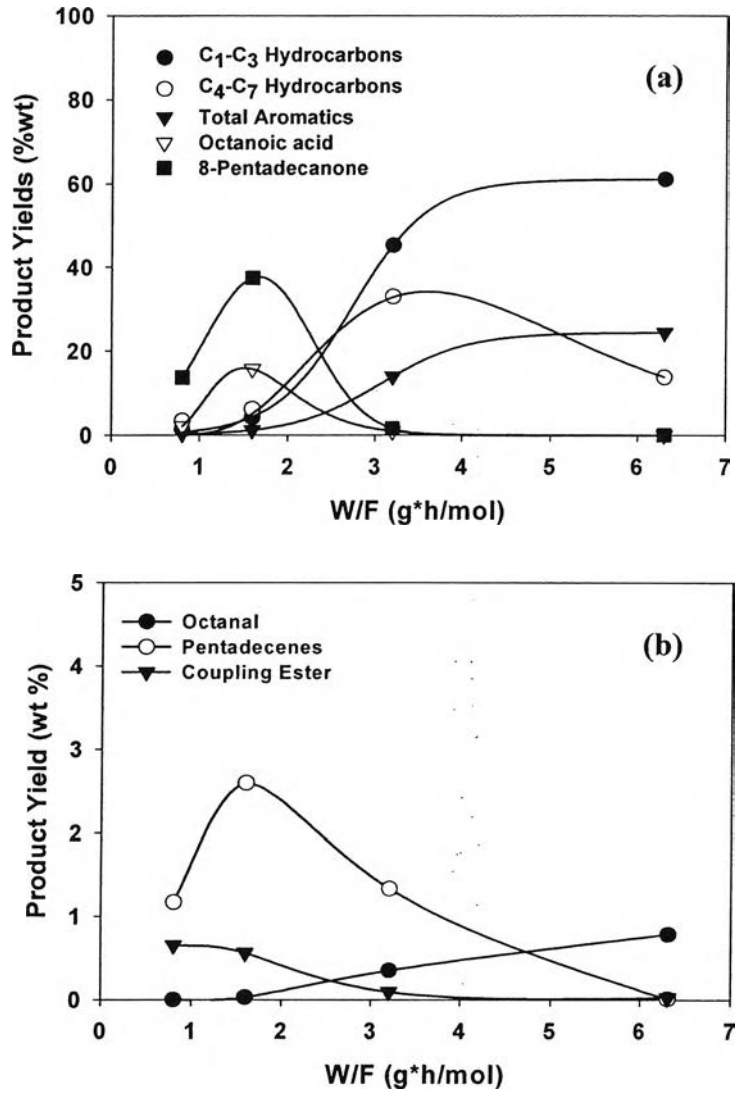

Figure 5.2 Product yield of (a) major products and (b) minor products obtained from the reaction of methyl octanoate on the Zn/H-ZSM5 as a function of W/F at 773 K.

5 .4.2 Conversion of n-Octane

To compare with the trends observed using methylester as a feed, we conducted a parallel study with n-octane, under the same conditions used for the FAME, i.e. gas phase, 773 K, atmospheric pressure, W/F from 0.8 to 25.4 $g_{cat}.h/mol_{nC8}$, H_2 to feed molar ratio of 6:1. The n-octane conversion curves as a function of time on stream over the H-ZSM5 and Zn/H-ZSM5 catalysts are reported

in Figure 5.3. Much better stability with time on stream was observed for n-octane on both catalysts than for the FAME. A slightly lower activity was observed for the Zn/H-ZSM5 compared to the H-ZSM5 catalyst. This lower activity parallels the lower Brønsted acidity of the Zn-containing catalyst, but more important, a significant difference is observed in the selectivity to aromatics.

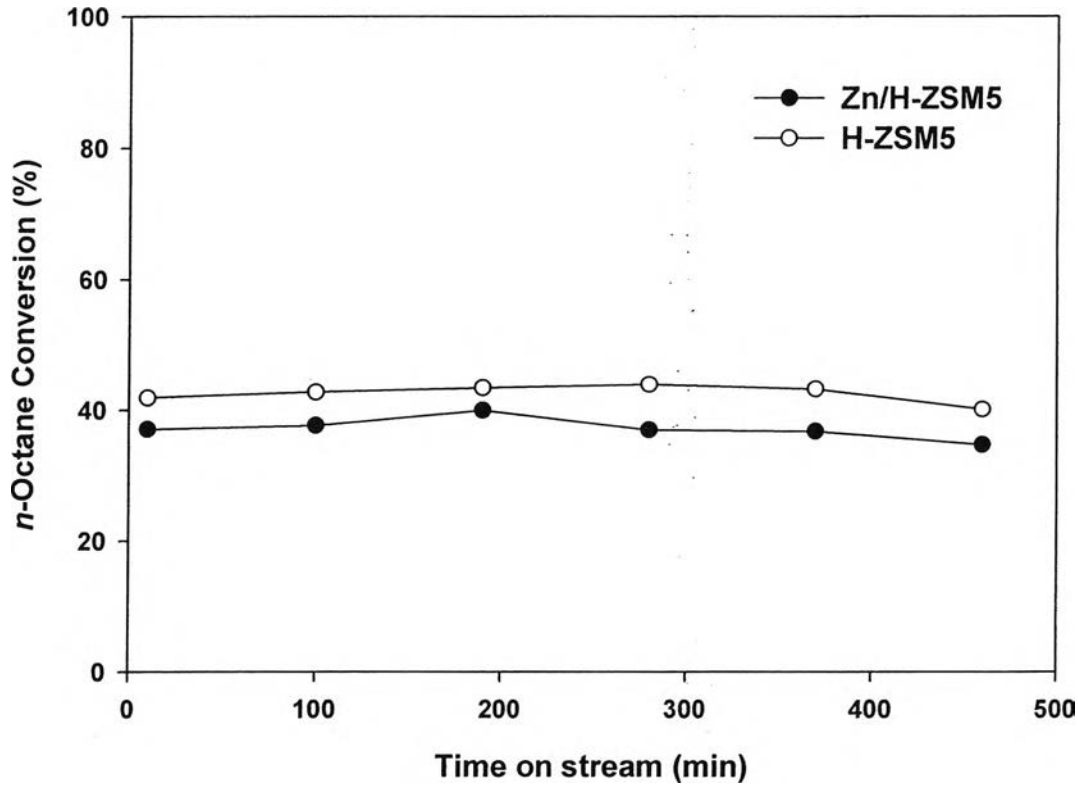

Figure 5.3 Conversion of n-octane over the H-ZSM5 and the Zn/H-ZSM5 catalysts as a function of time on stream at 773 K under atmospheric pressure with W/F = 3.2 g*h/mol.

As shown in Table 5.4, at about the same level of total conversion, the selectivity to aromatics over the Zn/H-ZSM5 is almost an order of magnitude higher than over the H-ZSM5, in agreement with previous studies on aromatization of light alkanes [14-19]. Several explanations have been given in the literature to interpret this effect. These explanations include the acceleration of specific steps in the mechanism such as the alkane activation via dissociative adsorption over Zn sites, the dehydrogenation of the alkane, the direct dehydrocyclization step, or modification of the surface fugacity of hydrogen under reaction conditions, or even by promoting.

Table 5.4 Product distributions from the reaction of n-octane on the H-ZSM5 and Zn/H-ZSM5 catalysts

	H-ZSM5		**Zn/H-ZSM5**	
Time on stream (min)	10	460	10	460
Conversion (%)	41.9	40.2	37.1	34.3
Product Selectivity (wt%)				
Methane	0.5	0.5	1.1	1.0
C_2	12.1	11.5	9.8	9.5
C_3	40.9	40.3	30.4	31.0
C_4	31.9	33.0	38.3	38.9
C_5	11.0	11.5	9.4	9.6
C_6	2.4	2.3	2.1	1.8
Benzene	0.1	0.1	1.5	1.6
Toluene	0.6	0.5	4.5	4.1
C_8 aromatics				
Ethylbenzene	0.0	0.0	0.3	0.3
m-Xylene	0.3	0.2	1.9	1.7
p-Xylene	0.2	0.1	0.7	0.5
o-Xylene	0.0	0.0	0.0	0.0

Reaction Conditions: 773 K, 1 atm, W/F = 3.2 g*h/mol, and H_2:Feed = 6:1 molar ratio

The strong promoting effect of Zn in the aromatization of light alkanes contrasts with the small differences observed between Zn/H-ZSM5 and H-ZSM5 when using FAME as a feed. Another interesting difference between the products obtained with the n-octane feed from those obtained with the FAME is the type of aromatics. That is, while the aromatics obtained from FAME contained significant amounts of C_8 and C_{9+} aromatics, those obtained from n-C_8 are dominated by benzene and toluene.

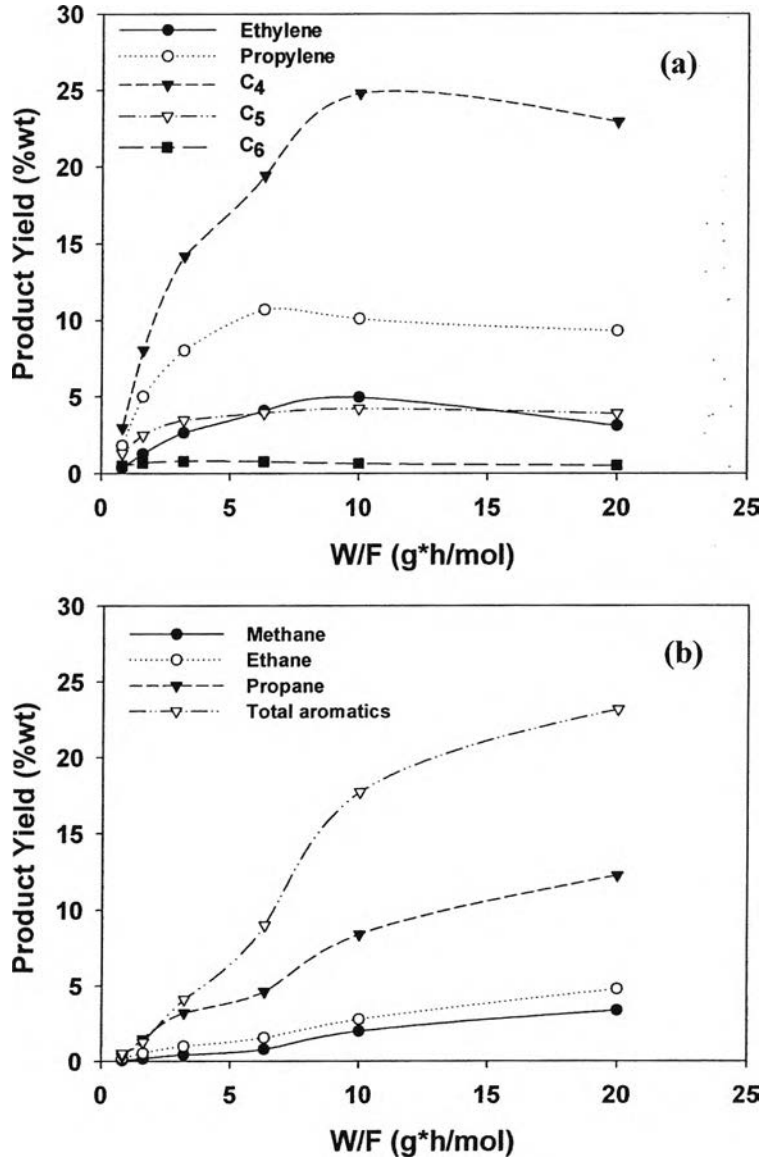

Figure 5.4 Product yield of (a) primary products and (b) secondary products obtained from the reaction of n-octane on the Zn/H-ZSM5 as a function of W/F at 773 K.

Figures 5.4 (a) and 5.4 (b) show the product distribution of the n-octane reaction over the Zn/H-ZSM5 catalyst as a function of contact time (W/F). It is seen that the yields of C_1-C_4 cracking products increase rapidly at low W/F, then reach a plateau or start being consumed. The formation of aromatics increases more slowly with W/F. As previously discussed [13] both the product distributions and their evolution with space time show that aromatics are secondary products, resulting from the oligomerization and cyclization of the smaller molecules produced by cracking. In our previous work on the reaction of n-octane over the H-ZSM5 we showed the the evolution of product distribution as a function of W/F, and the trend reported in that study is very similar to that shown here for Zn/H-ZSM5 [13]. This similarity indicates that the presence of zinc in the Zn/H-ZSM5 catalyst does not provide alternative reaction paths for the aromatization of n-octane, but it simply makes the secondary aromatization more effective.

A comparison is made in Table 5.5 for distribution of products obtained at low conversions over the two catalysts and with the two different feeds. It is clear that with the n-octane feed, practically no aromatics are formed at low conversion on either of the two catalysts, but only cracking products are obtained. By contrast, when the feed is the FAME, the condensation products dominate in the distribution and even at low conversions some aromatics are obtained.

Table 5.5 Product distributions from the reactions of methyl octanoate and n-octane on the H-ZSM5 and Zn/H-ZSM5 at low conversion

	n-Octane		**Methyl Octanoate**	
	H-ZSM5	Zn/H-ZSM5	H-ZSM5	Zn/H-ZSM5
Conversion (%)	7.7	7.5	7.2	10.1
Product Selectivity (wt%)				
Methane	0.7	0.8	1.4	1.4
C_2	10.3	7.4	1.8	5.9
C_3	35.1	28.4	3.7	4.9
C_4	32.7	39.5	0.6	0.5
C_5	15.3	17.3	0.5	1.2
C_6	5.9	6.3	1.0	2.8
C_7	0.0	0.0	9.4	16.3
Benzene	0.0	0.3	0.1	0.3
Toluene	0.0	0.0	0.1	0.2
C_8 aromatics				
Ethylbenzene	0.0	0.0	0.1	0.3
m-Xylene	0.0	0.0	0.2	0.5
p-Xylene	0.0	0.0	0.1	0.3
o-Xylene	0.0	0.0	0.1	2.1
C_9+ aromatics	0.0	0.0	2.3	1.5
Total Aromatics	0.0	0.3	3.0	5.2
Octanal	0.0	0.0	3.0	17.8
Octanoic acid	0.0	0.0	31.2	30.6
Coupling Products	0.0	0.0	44.4	13.4

Reaction Conditions: 773 K, 1 atm, and H_2:Feed = 6:1 molar ratio

Another indication of the differences between the two catalysts and the two reactants arises from the analysis of the cracking product distribution as a function of conversion. Figure 5.5 compares the distribution of cracking products (C_1-C_7) at three levels of conversions over Zn/H-ZSM5 and H-ZSM5 for the two feeds (n-C_8 and FAME). It is interesting to note that in the n-octane reaction (Figure 5.5 (a)) the distributions are very similar, regardless of conversion level or catalyst used. The dominant cracking products are C_3 and C_4, indicating that the n-C_8 alkane is preferentially cracked near the middle of the chain in both catalysts. There is a slight shift to longer chain fragments in the Zn-modified catalyst, which might be ascribed to the lower density of acid sites. By contrast, in the conversion of the FAME (Figure 5.5 (b)), the dominant cracking products are C_7 and C_2, the latter dominates at low conversions while the former dominates at high conversions. This trend indicates that the initial formation of hydrocarbons occurs near the oxygenated end via decarbonylation/decarboxylation as previously discussed [13]. This type of reactions produce olefins and alkanes with one carbon atom less than the original fatty acid chain in the ester [7,28]. In the case, of methyloctanoate, the decarbonylation/ decarboxylation product first obtained is C_7. S ubsequently, at higher conversion levels this long hydrocarbon chain can be further cracked into smaller fragments, as observed in Figure 5.5 (b).

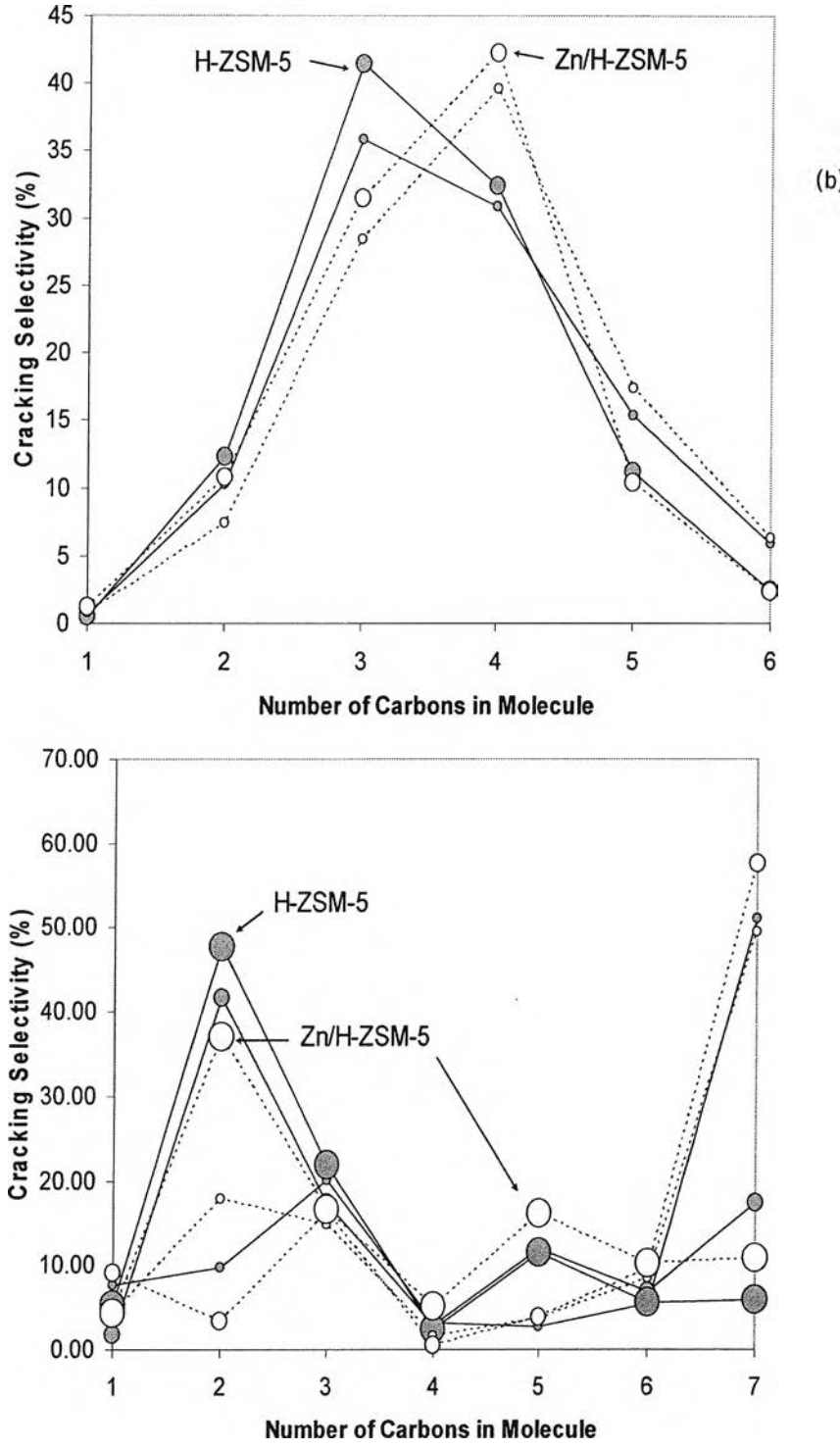

Figure 5.5 Distribution of cracking products from (a) n-octane and (b) methyl-octanoate over H-ZSM5 (open symbols) and Zn/H-ZSM5 (full symbols). Conversion levels are indicated by the size of the symbol. Small (~10%); Medium (~40%); and Large (~100%).

To better visualize the selectivity trends, we have plotted in Figure 5.6 the yield of non-aromatic hydrocarbons as a function of the yield of aromatics from methyl octanoate and from n-octane over both H-ZSM5 and Zn/H-ZSM5 catalysts. This type of yield-yield graphs are particularly useful when catalysts of different intrinsic activity are compared and the reactions involved include parallel and sequential paths. That is, this graph allows us to compare the amount of side products obtained to reach a given yield of the desired product. For example, in the case of FAME conversion, the yield of non-aromatic hydrocarbon increases with increasing total aromatics but at conversions high enough some of these products are converted into aromatics. Therefore, at high aromatics yields (high conversions) the selectivity is rather high, but quickly drops as the catalyst deactivates or the W/F decreases. The best catalyst would be one in which the maximum yield of non-aromatic hydrocarbons is relatively low, so the loss in selectivity by activity drop would not be as pronounced. As seen in Figure 5.6, when the feed is the FAME, both catalysts, Zn/H-ZSM5 and H-ZSM5, seem to follow the same trend, suggesting that the addition of the Zn cation to H-ZSM5 does not improve significantly the aromatization activity in the conversion of methylesters. By contrast, the effect of Zn in aromatizing alkanes is clearly seen when comapring the yield-Vs-yield patterns for the case of n-octane feed. The greater effectiveness of Zn/H-ZSM5 for converting smaller fragments into aromatic molecules is noticeable. Much less non-aromatics (i.e. short olefins and alkanes) are produced over Zn/H-ZSM5 than over H-ZSM5 to reach a given yield of aromatics; or, conversely, with a given yield of non-aromatic hydrocarbon much more aromatics are formed on the Zn-modified catalyst.

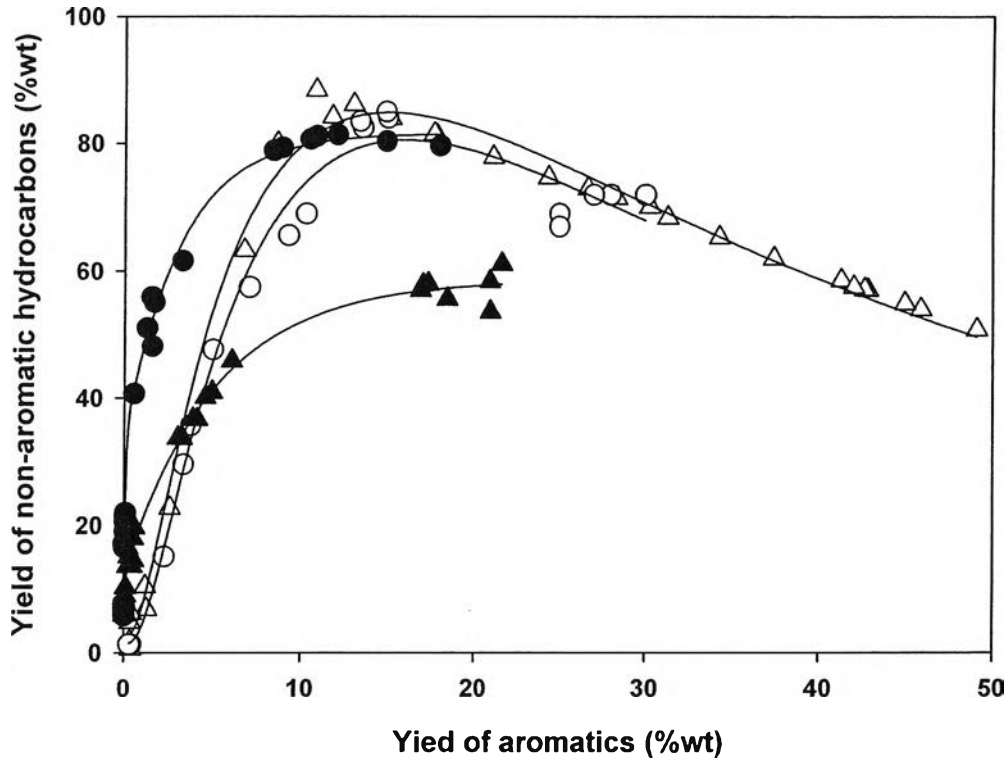

Figure 5.6 Yield of non-aromatic hydrocarbons Vs. Yield of aromatic hydrocarbons for the reactions of n-octane (full symbols) and methyl octanoate (open symbols) over Zn/H-ZSM5 (triangle) and H-ZSM5 (circle) catalysts at 773 K and varying W/F and times on stream, which result in varying levels of aromatic yields.

An interesting trend that can be observed in Figure 5.7 is the variation of the percentage of o-xylene in total aromatics as a function of yield of total aromatics. o-Xylene is an interesting product to follow since it can be formed by direct ciclization of an 8-carbon chain. That is, we have previously shown [29] that when an n-octane molecule aromatizes by direct ring closure it only forms o-xylene (connecting the second and seventh C atoms in the chain) or ethylbenzene (connecting the first and the sixth C). The fact that no o-xylene is seen in the aromatic product at low conversions when the feed is n-octane, but only at high conversions, indicates that with this feed direct ring closure does not occur, as previously indicated [13], but rather it is formed by isomerization of the other xylenes. By contrast, a very interesting trend is observed when the feed is the methyl

ester. It is observed that on both catalysts, Zn/H-ZSM5 and H-ZSM5, the percentage of o-xylene at low conversions is very high, which would indicate that a direct ring closure occurs with the oxygenated molecule. It is expected that, with the formation of the various condesantion products mentioned above and their subsequent cracking, different aromatization paths take place in the reaction of methyloctanoate. However, a preferential ring closure is likely to occur, involving the H atom bonded to the C in the α position relative to the carbonyl group, which typically displays high activity. This important result gives strong support to the idea that aromatization on oxygenated compounds can proceed before deoxygenation and it is favored by the presence of a carbonyl group. After the ring is closed, the carbonyl can quickly convert by the acid-catalyzed tautamerization into the enol form, which in turn can be dehydrated and further dehydrogenated to form the observed o-xylene.

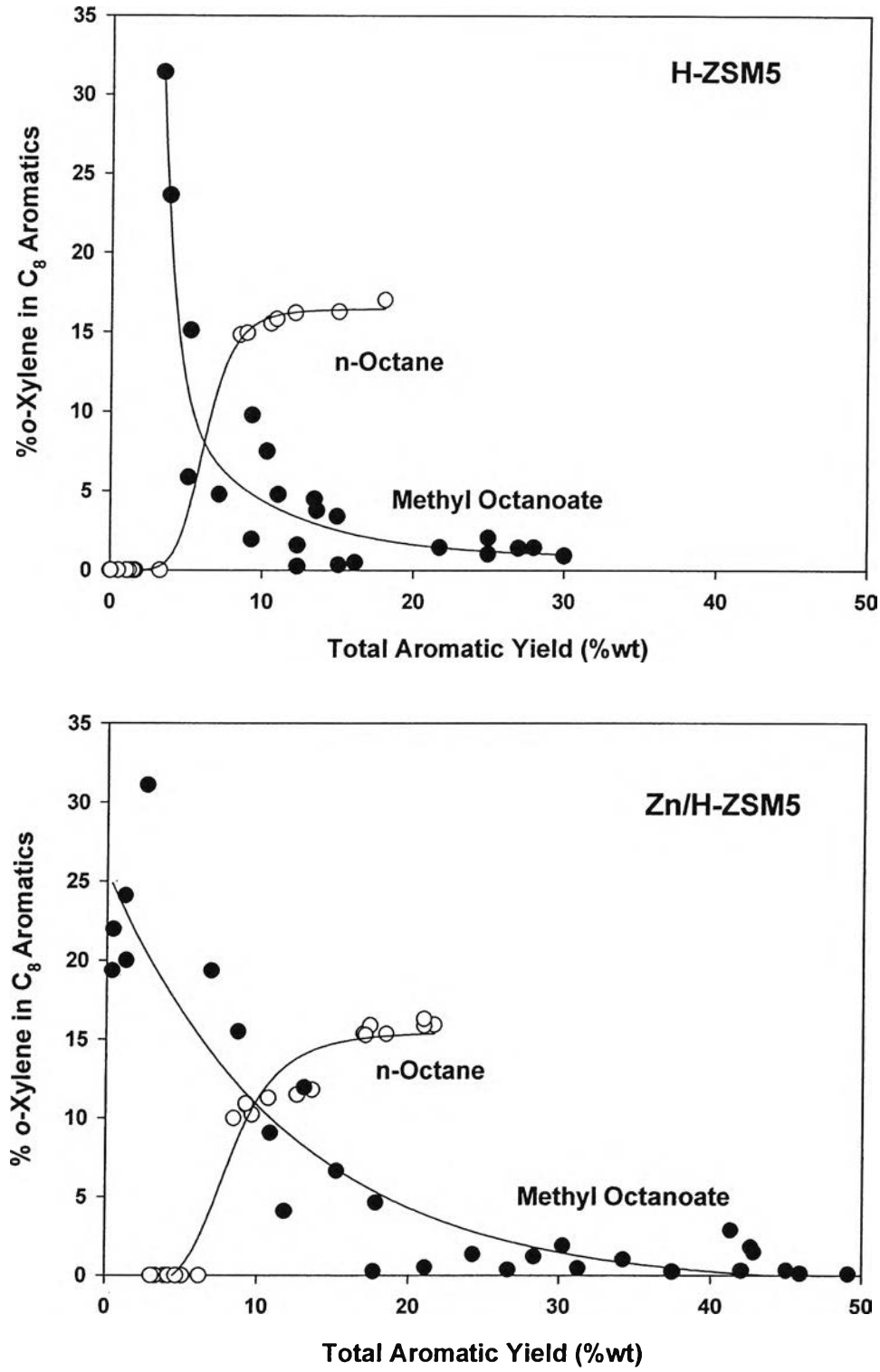

Figure 5.7 Percentage of o-Xylene in total aromatics as a function of yield of total aromatics obtained over H-ZSM5 (top) and Zn/H-ZSM5 (bottom) using as a feed n-octane (open symbols) or methyl octanoate (full symbols).

5.5 Conclusions

The conversion of methyl octanoate, a model fatty acid methyl ester, has been studied on Zn/H-ZSM5 and H-ZSM5 catalysts. Deoxygenation, coupling, cracking, and aromatization reactions take place under the reaction conditions investigated. These reactions are relevant to the refining of fuels derived from biomass containing triglycerides, such as vegetable oils and algae. The main conclusions of the study are the following:

(a) The addition of Zn to H-ZSM5 catalysts does not result in a significant improvement in the aromatization capacity of the catalyst. The methylester conversion includes condensation reactions (ketonization, esterification) that lead to the formation of larger compounds that subsequently deoxygenate and crack forming aromatics. The presence of Zn does not seem to greatly enhance any of these steps.

(b) By contrast, a significant enhancement in aromatization activity was observed for the reaction of n-octane over the Zn/H-ZSM5. In this case, the presence of Zn makes the catalyst more effective for converting the smaller molecular fragments (i.e. short olefins) into aromatics.

(c) The deoxygenation of methyl octanoate on the Zn/H-ZSM5 catalyst takes place through the same reaction pathways as that on the H-ZSM5. That is, the addition of Zn does not provide any alternative reaction routes.

(d) One of the dominant aromatization paths involved in the reaction of methyloctanoate is the direct ring closure forming o-xylene as main product. This path most probably occurs via activation of the H atom bonded to the C in the α position relative to the carbonyl group. That is, oxygenated compounds maybe aromatized before deoxygenation.

5.6 Acknowledgements

This work has been partially supported by the Oklahoma Secretary of Energy, and the Oklahoma Bioenergy Center, the Thailand Research Fund (TRF) under the Royal Golden Jubilee Ph.D. programs, Center for Petroleum, Petrochemicals, and Advanced Materials (PPAM), and the Petrochemical and

Environmental Catalysis Research Unit of Ratchadapiseksompote Endowment, Chulalongkorn University.

5.7 References

[1] D. E. Lopez, K. Suwannakarn, D. A. Bruce, J. G. Goodwin Jr., *J. Catal.* 247 (2007) 43.

[2] I. N. Martynov, A. Sayari, *Appl. Catal. A* 339 (2008) 45.

[3] D. G. Aranda, R. T. P. Santos, N. C. O. Tanpanes, A. L. D. Ramos, O. A. C. Antunes, *Catal. Lett.* 122 (2008) 20.

[4] G. Knothe, *Fuel Process. Technol.*, 86 (2005) 1059.

[5] G. Knothe, A. C. Matheaus, T.W. Ryan III, *Fuel* 82 (2003) 971.

[6] G. Knothe, *Energy Fuels* 22 (2008) 1358.

[7] P.Maki-Arvela, I. Kubickova, M. Snare, K. Eranen, D.Y. Murzin, *Energy and Fuels* 21(2007) 30.

[8] O. I. Senol, T. R. Viljava, A. O. I. Krause, *Catal. Today* 100 (2005) 331.

[9] O. I. Senol, T. R. Viljava, A. O. I. Krause, *Catal. Today* 106 (2005) 186.

[10] E. Furimsky, *Appl. Catal. A.* 199 (2000) 147.

[11] J. D. Adjave, N. N. Bakhshi, *Fuel Proc. Techno.* 45 (1995) 161.

[12] J. D. Adjave, N. N. Bakhshi, *Energy Fuel* 9 (1995) 1605.

[13] T. Danuthai, S. Jongpatiwut, T. Rirksomboon, S. Osuwan, D.E. Resasco, *App. Catal A.* 361 (2009), 99.

[14] T. Mole, J. R. Anderson, *Appl. Catal.* 17 (1985) 141.

[15] J. A. Biscardi, E. Iglesia, *J. Catal.* 182 (1999) 117.

[16] Y.G. Kolyagin, V.V. Ordomsky, Y.Z. Khimyak, A.I. Rebrov, F. Fajula, I.I. Ivanova, J. Catal. 238 (2006) 122.

[17] N. Viswanadham, A. R. Pradhan, N. Ray, S.C. Vishnoi, U. Shanker, T.S. R. Prasada Rao, *App. Catal. A* 137 (1996) 225.

[18] V.B. Kazansky, A.I. Serykh, E.A. Pidko, *J. Catal.* 225 (2004) 369.

[19] V.B. Kazansky, E.A. Pidko, *J. Phys. Chem. B* 109 (2005) 2103.

[20] R. J. Argauer, G. R. Landolt, US Patent 3 702 886 (1972).

[21] D. J. Parrillo, A. T. Adamo, G. T. Kokotailo, R. J. Gorte, *Appl. Catal.*, 67 (1990) 107.

[22] C. A. Emeis, *J. Catal.* 141 (1993) 347.

[23] Y. Ono, *Catal. Rev.-Sci. Eng.* 34 (1992) 179.

[24] A. Smiešková, E. Rojasová, P. Hudec, L. Šabo, *App. Catal A.* 268 (2004) 235.

[25] J.A. Martens, M. Wydoodt, P. Espeel, P.A. Jacobs *Stud. Surf. Sci. Catal.*, 78 (1993) 527.

[26] E. L. Kunkes, D. A. Simonetti, R. M. West, J. C. Serrano-Ruiz, C. A. Gärtner, J. A. Dumesic, *Science*, 322 (2008) 417.

[27] J. N. Chheda and J. A. Dumesic, *Catal. Today* 123 (2007) 59.

[28] I. Kubickova, M. Snare, K. Eranen, P. Maki-Arvela, D. Y. Murzin, *Catal. Today*, 106 (2005) 197.

[29] S. Jongpatiwut, S. Trakarnroek, T. Rirksomboon, S. Osuwan, D. E. Resasco, *Catal. Lett.* 100 (2005) 7.